

A New 3D Supramolecular Manganese(II) Complex Constructed from Benzimidazole-5,6-dicarboxylate and Oxalate: Synthesis, Structural, and Magnetic Properties

Jin-Peng Geng,^[a] Zhao-Xi Wang,^{*[a]} Qiong-Fang Wu,^[a] Ming-Xing Li,^[a,c] and Hong-Ping Xiao^{*[b]}

Keywords: Manganese; Benzimidazole-5,6-dicarboxylate acid; X-ray diffraction; IR spectroscopy; Magnetic properties

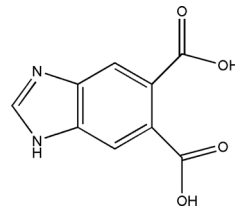
Abstract. A new manganese(II) complex $[\text{Mn}_3(\text{bidc})_2(\text{C}_2\text{O}_4)(\text{H}_2\text{O})_{10}]$ (**1**) (bidc = benzimidazole-5,6-dicarboxylate) was synthesized and characterized by X-ray crystallography. X-ray diffraction shows that complex **1** has a neutral, one-dimensional (1D) brick wall chain structure. With the intramolecular and intermolecular hydrogen bonding in-

teractions, the adjacent chains are joined into a 3D supramolecular architecture. IR spectroscopy and variable temperature magnetic susceptibility measurements were made, which indicated weak antiferromagnetic coupling between the Mn^{II} ions in complex **1**.

Introduction

In the recent years, coordination compounds with the ligand benzimidazole-5,6-dicarboxylic acid (H_2bidc) (Scheme 1) were of great interest in the field of crystal engineering due to their novel and diverse topologies and interesting features, such as magnetic and optical properties.^[1–6] The H_2bidc ligand attracted our attention because of its multifunctional coordination modes, as it should be able to bond to metal ions in different fashions by the carboxylate groups and imidazole nitrogen atoms, thus allowing for the formation of novel polymeric structures. For instance, Li et al. used 4d–4f metal ions to synthesize a series of novel 3D coordination polymers with “pcu” topology.^[7]

In our previous works, we have employed H_2bidc as bridging ligand to construct several 2D and 3D polymers based on lanthanide secondary building units.^[8] It is noted that all of the coordination polymers composed of H_2bidc were prepared by hydrothermal reactions because of its poor water solubility. Up to now, only two complexes with the H_2bidc ligand have been



Scheme 1. Chemical structure of H_2bidc .

obtained by normal methods.^[9, 10] In order to get metal-organic coordination polymers based on H_2bidc by normal methods, we investigated the addition of oxalic acid as an auxiliary bridging ligand to the reaction mixture. Fortunately, we harvested a new manganese(II) complex with benzimidazole-5,6-dicarboxylate and oxalate ligands, $[\text{Mn}_3(\text{bidc})_2(\text{C}_2\text{O}_4)(\text{H}_2\text{O})_{10}]$ (**1**). Herein, we reported the synthesis, crystal structure and magnetic properties of **1**.

Results and Discussion

Synthesis, IR Spectroscopy, and Thermal Stability

Complex **1** was obtained by slow evaporation of a mixed solution of $\text{MnSO}_4 \cdot \text{H}_2\text{O}$ with H_2bidc and oxalic acid. It is interesting that the ratio of H_2bidc and oxalic acid plays a vital role in the formation of **1**. To obtain the desired compound in good quality, the H_2bidc -to- $\text{H}_2\text{C}_2\text{O}_4$ ratio should be strictly controlled between 5:1 and 6:1. We speculate that there may be a competition between H_2bidc and oxalic acid in the process of formation of complex **1**.

In the IR spectrum of complex **1** (Supporting Information Figure S1), no absorption signal near 1700 cm^{-1} for $-\text{COOH}$ is observed, which indicates that the carboxyl groups of H_2bidc

* Prof. Dr. Z.-X. Wang
Fax: +86-21-66132797
E-Mail: zxwang@shu.edu.cn

* Prof. Dr. H.-P. Xiao
E-Mail: hp_xiao@wzu.edu.cn

[a] Department of Chemistry
College of Science
Shanghai University
Shanghai 200444, P. R. China

[b] College of Chemistry and Materials Engineering
Wenzhou University
Wenzhou 325035, P. R. China

[c] State Key Laboratory of Coordination Chemistry
Nanjing University
Nanjing 210093, P. R. China

Supporting information for this article is available on the WWW under <http://dx.doi.org/10.1002/zaac.201000295> or from the author.

are deprotonated. The strong signals around 1633 cm^{-1} and 1362 cm^{-1} are characteristic for the asymmetric and symmetric vibrations of the carboxylate group.^[11, 12] The characteristic absorptions of $-\text{OH}$ (water) and $\text{N}-\text{H}$ (ligand H_2bidc) are observed at 3337 cm^{-1} and 3166 cm^{-1} , respectively. The absorptions of the asymmetric and symmetric vibrations of the oxalate group are observed at around 1549 cm^{-1} and 1416 cm^{-1} , which suggest that oxalate adopts a chelating bidentate coordination mode.^[13]

In order to examine the thermal stability of complex **1**, thermal gravimetric analyses (TGA) were carried out under nitrogen. The TGA curve of **1** reveals a continuous weight loss of 21.1 % below $180\text{ }^{\circ}\text{C}$, which is attributed to the loss of coordinated water molecules (calcd. 21.4 %) (Supporting Information, Figure S2). The following weight loss in the tem-

perature range of $180\text{ }^{\circ}\text{C}$ to $737\text{ }^{\circ}\text{C}$ corresponds to the decomposition of oxalate and bidc^{2-} ligands. Finally, the residue is MnO_2 (found 31.4 %, calcd. 31 %).

Structural Description

X-ray diffraction analysis reveals that complex **1** is a neutral, one-dimensional brick wall chain coordination polymer. A view of the coordination environment of the Mn^{II} ions in **1** with atom labeling is shown in Figure 1. The asymmetric unit consists of one and a half crystallographically independent Mn^{II} ions, a bidc^{2-} dianion, half an oxalate dianion, and five coordinated water molecules. The $\text{Mn}1$ atom is hexacoordinated, showing a distorted octahedral arrangement with five oxygen atoms and one nitrogen atom from an oxalate molecule, three water molecules and a bidc^{2-} dianion, respectively. Compared to $\text{Mn}1$, $\text{Mn}2$ is also hexacoordinated with two carboxylate oxygen atoms ($\text{O}4$, $\text{O}4\text{B}$, symmetry code: B: $-x+1$, $-y+1$, $-z+1$) from two bidc^{2-} dianions, and four oxygen atoms ($\text{O}10$, $\text{O}10\text{B}$, $\text{O}11$, and $\text{O}11\text{B}$) from four coordinated water molecules. The $\text{Mn}-\text{O}$ bond lengths range from $2.095(2)$ to $2.287(2)\text{ \AA}$ (Table 1), which are similar to those observed for other Mn^{II} complexes.^[14] In the crystal structure, the bidc^{2-} ligand acts as a μ_2 -bridge and connects two Mn^{II} ions through one oxygen atom of the monodentate carboxylate group and one nitrogen atom of the benzimidazole ring. This coordination mode of the bidc^{2-} ligand has just been reported for cobalt complexes.^[9] Oxalate as bis(bidentate) ligand links the atoms $\text{Mn}1$ and $\text{Mn}1\text{A}$ (symmetry code: A: $-x+1$, $-y+1$, $-z$) by its oxygen atoms to form a dinuclear unit. This mode was also reported for lanthanide complexes based on H_2bidc and oxalate ligands.^[15] Furthermore, the dinuclear unit and the $\text{Mn}2$ atom are linked by μ_2 - bidc^{2-} bridges to build a 1D chain along the *c* axis (Figure 2).

In the crystal structure, intramolecular and intermolecular hydrogen bonding interactions are observed (Table 2). There

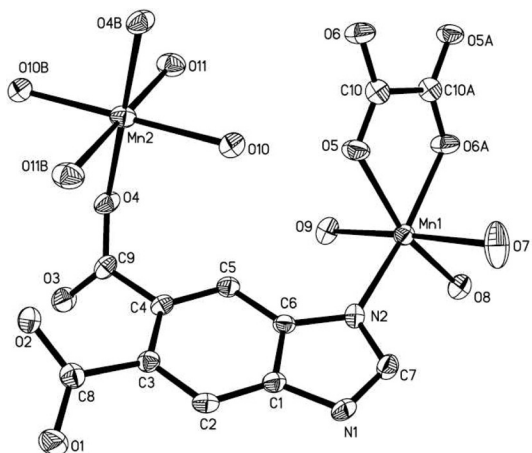


Figure 1. View of the coordinational environment of Mn^{II} ions in **1**, thermal ellipsoids at the 50 % probability level. All hydrogen atoms were omitted for clarity. Symmetry codes: A: $-x+1$, $-y+1$, $-z$; B: $-x+1$, $-y+1$, $-z+1$.

Table 1. Selected bond lengths / \AA and bond angles / $^{\circ}$ for **1**.

Mn1–O7	2.156(3)	Mn1–N2	2.188(3)
Mn1–O8	2.192(3)	Mn1–O9	2.194(3)
Mn1–O6A	2.206(2)	Mn1–O5	2.219(2)
Mn2–O4B	2.095(2)	Mn2–O4	2.095(2)
Mn2–O11B	2.182(3)	Mn2–O11	2.182(3)
Mn2–O10	2.287(2)	Mn2–O10B	2.287(2)
O7–Mn1–N2	89.24(11)	O7–Mn1–O8	84.71(11)
N2–Mn1–O8	104.33(11)	O7–Mn1–O9	172.10(10)
N2–Mn1–O9	93.74(10)	O8–Mn1–O9	87.47(10)
O7–Mn1–O6A	88.38(11)	N2–Mn1–O6A	167.34(10)
O8–Mn1–O6A	87.83(10)	O9–Mn1–O6A	90.26(10)
O7–Mn1–O5	96.27(11)	N2–Mn1–O5	93.11(10)
O8–Mn1–O5	162.56(10)	O9–Mn1–O5	90.88(10)
O6A–Mn1–O5	74.81(9)	O4B–Mn2–O4	180.0
O4B–Mn2–O11B	90.57(10)	O4–Mn2–O11B	89.43(10)
O4B–Mn2–O11	89.43(10)	O4–Mn2–O11	90.57(10)
O11B–Mn2–O11	180.00(12)	O4B–Mn2–O10	77.93(9)
O4–Mn2–O10	102.07(9)	O11B–Mn2–O10	86.50(9)
O11–Mn2–O10	93.50(9)	O4B–Mn2–O10B	102.07(9)
O4–Mn2–O10B	77.93(9)	O11B–Mn2–O10B	93.50(9)
O11–Mn2–O10B	86.50(9)	O10–Mn2–O10B	180.0

Symmetry codes: A: $-x+1$, $-y+1$, $-z$; B: $-x+1$, $-y+1$, $-z+1$.

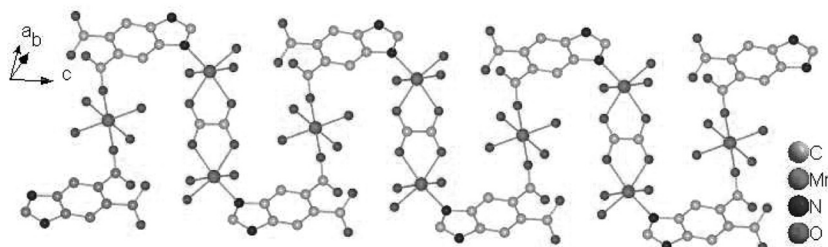


Figure 2. The 1D infinite structure of **1**. Hydrogen atoms were omitted for clarity.

exist two N–H···O hydrogen bonds (N1–H1···O10^a, N1–H1···O11^b, symmetry code: a: $-x+1, -y, -z+1$; b: $x, y-1, z$) with the oxygen atoms from two coordinated water molecules of Mn²⁺, respectively. Between the coordinated aqua oxygen atoms the intermolecular hydrogen bond O10–H10A···O9^c (symmetry code: c: $x+1, y, z$) is observed. Four O–H···O intermolecular hydrogen bonds (O7–H7B···O1^a, O8–H8B···O1^e, O9–H9A···O3^g, and O11–H11B···O3^g, symmetry code: e: $-x, -y, -z+1$; g: $-x, -y+1, -z+1$) are formed between coordinated aqua oxygen atoms and uncoordinated carboxylate oxygen atoms. The O9–H9B···O6^f (symmetry code: f: $x-1, y, z$) intermolecular hydrogen bond is generated between the coordinated aqua atom O9 and the coordinated carboxylate atom O6. Meanwhile, intramolecular hydrogen bonding interactions are found between coordinated aqua oxygen atoms and uncoordinated carboxylate oxygen atoms (O7–H7A···O2^d, O8–H8A···O2^d, O11–H11A···O2^h, symmetrical code: d: $x, y, z-1$; h: $-x+1, -y+1, -z+1$), and between the coordinated aqua atom O10 and the aqua atom O5. All above hydrogen bonding interactions may enhance the stability of the structure of complex **1** and generate a 3D supramolecular architecture (Figure 3).

Table 2. Hydrogen bonding parameters for **1** /Å and °.

D–H···A	<i>d</i> (D–H)	<i>d</i> (H···A)	<DHA	<i>d</i> (D···A)
N1–H1···O10 ^a	0.86	2.27	146.4	3.027(4)
N1–H1···O11 ^b	0.86	2.39	130.4	3.015(4)
O7–H7B···O1 ^a	0.85	1.91	150.8	2.683(4)
O10–H10A···O9 ^c	0.85	2.10	174.4	2.943(4)
O7–H7A···O2 ^d	0.85	1.94	147.6	2.695(4)
O(8)–H8A···O2 ^d	0.85	2.15	159.2	2.958(4)
O8–H8B···O1 ^e	0.85	1.98	144.8	2.717(4)
O9–H9B···O6 ^f	0.85	1.89	167.6	2.722(3)
O9–H9A···O3 ^g	0.85	1.94	160.0	2.753(3)
O11–H11B···O3 ^g	0.85	1.95	159.2	2.758(4)
O10–H10B···O5	0.85	2.19	138.2	2.877(3)
O11–H11A···O2 ^h	0.85	1.92	159.3	2.733(4)
Symmetry codes: a: $-x+1, -y, -z+1$; b: $x, y-1, z$; c: $x+1, y, z$; d: $x, y, z-1$; e: $-x, -y, -z+1$; f: $x-1, y, z$; g: $-x, -y+1, -z+1$; h: $-x+1, -y+1, -z+1$				

Magnetic Properties

Magnetic susceptibility measurements of a crystalline sample of **1** were carried out using a Quantum Design MPMS-XL7 SQUID magnetometer in an applied magnetic field of 2 KOe in the temperature range 1.8–300 K. Variable-temperature

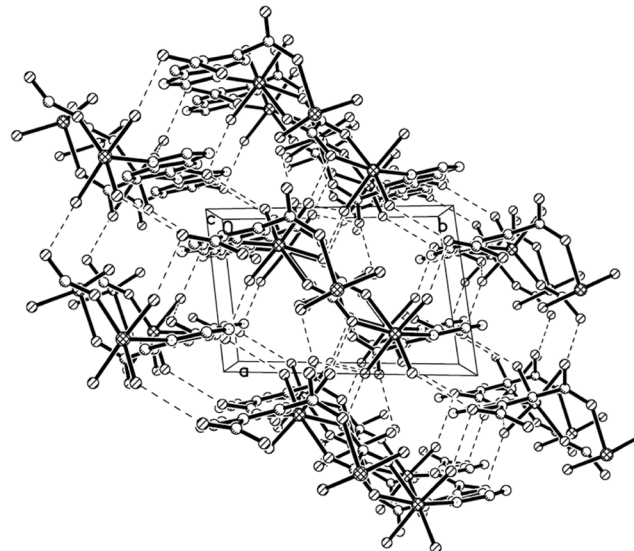


Figure 3. View of 3D supramolecular architecture of **1** along the *c* axis. The dotted lines represent hydrogen bonding interactions.

magnetic susceptibility in the forms of $1/\chi_M$ and $\chi_M T$ versus *T* in the range of 300 to 1.8 K is shown in Figure 4. At room temperature, the $\chi_M T$ value is 13.54 emu·K·mol⁻¹, which is slightly higher than the spin-only value (13.14 emu·K·mol⁻¹) of three isolated Mn^{II} (*S* = 5/2) ions assuming *g* = 2.0. When the temperature is lowered, $\chi_M T$ smoothly decreases and reaches 0.54 emu·K·mol⁻¹ upon cooling to 1.8 K, which is typical for antiferromagnetic interactions.^[16, 17] The magnetic susceptibility data follows the Curie–Weiss law with *C* = 14.08 emu·K·mol⁻¹ and θ = -10.5 K. The *C* value corresponds to the value expected for the manganese(II) ion with *g* = 2.07. These results also suggest antiferromagnetic interaction between the manganese(II) ions. Compared to the oxalate bridge, the coupling interaction between the manganese(II) ions mediated by the bidc²⁻ ligand might be negligible.^[2, 3] To estimate the magnitude of the antiferromagnetic coupling, the isotropic spin Hamiltonian $H = -2J(S_{Mn1}S_{Mn1A})$ was used for the dinuclear unit with $S_{Mn} = 5/2$, where *J* is the coupling constant mediated by oxalate bridges. When the isolated Mn^{II} ion is taken into account, the expression was written by the Kambe method^[18] as follows:

$$\chi_M = \frac{2N\beta^2 g^2}{kT} \times \frac{\exp(2J/kT) + 5\exp(6J/kT) + 14\exp(12J/kT) + 30\exp(20J/kT) + 55\exp(30J/kT)}{1 + 3\exp(2J/kT) + 5\exp(6J/kT) + 7\exp(12J/kT) + 9\exp(20J/kT) + 11\exp(30J/kT)} + \frac{35N\beta^2 g^2}{12kT} \quad (1)$$

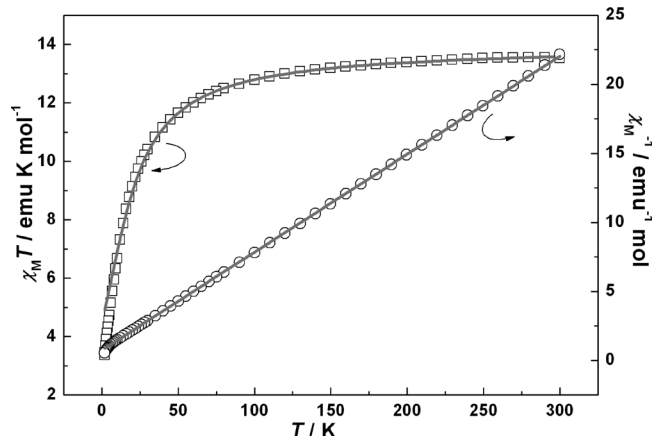


Figure 4. Temperature dependence of the $\chi_M T$ and $1/\chi_M T$ product for **1** at 2 KOe field. The solid line is the best fits obtained from the model described in the text.

With this equation, the calculated results in the temperature range from 35 to 300 K are $J = -1.50 \text{ cm}^{-1}$, and $g = 2.063$ with $R = \Sigma[(\chi_M T)_{\text{calc}} - (\chi_M T)_{\text{obs}}]^2 / \Sigma(\chi_M T)_{\text{obs}}^2 = 3.7 \times 10^{-4}$. The negative coupling constant indicates antiferromagnetic coupling between the neighboring Mn^{II} ions mediated by oxalate bridges, which are similar to those reported previously.^[19]

Conclusions

A new manganese(II) complex $[\text{Mn}_3(\text{bidc})_2(\text{C}_2\text{O}_4)(\text{H}_2\text{O})_{10}]_n$ with 3D supramolecular architecture was synthesized and characterized. The stability of the structure in the solid-state was strengthened by the intramolecular and intermolecular hydrogen bonding interactions. Magnetic analysis revealed antiferromagnetic coupling interactions between the Mn^{II} ions.

Experimental Section

Materials and Methods

All chemicals used during the course of this work were of reagent grade and used as received from commercial sources without further purification. Elemental analyses for carbon, hydrogen, and nitrogen were carried out with a Vario EL III elemental analyzer. Infrared spectra were recorded with a Nicolet A370 FT-IR spectrometer using KBr pellets in the 4000–400 cm^{-1} region. TGA experiment was performed with a Shimadzu DT-20B thermogravimetric analyzer from 20 to 800 °C at a heating rate of 10 °C·min⁻¹ in nitrogen. Variable-temperature magnetic susceptibility measurements were taken at an applied field of 2 KOe on a Quantum Design MPMS-XL7 SQUID magnetometer working in the temperature range of 300–1.8 K. The molar magnetic susceptibilities were corrected for the diamagnetism estimated from Pascal's tables and for the sample holder by previous calibration.

Preparation of $[\text{Mn}_3(\text{bidc})_2(\text{C}_2\text{O}_4)(\text{H}_2\text{O})_{10}]_n$ (1): Complex **1** was prepared by reaction of H₂bidc (0.16 mmol), oxalic acid (0.03 mmol), and MnSO₄·H₂O (0.3 mmol) in ethanol/water (v/v 1:1). Single crystals were obtained after two weeks in a yield of 21.1 % (based on Mn). Anal. calculated for C₂₀H₂₈Mn₃N₄O₂₂: C 28.55; H 3.35; N 6.66 %; found: C 28.19; H 3.62; N 6.90 %. IR (KBr): $\tilde{\nu} = 3337$ (m), 3166 (s), 1633 (s), 1549 (s), 1468 (s), 1416 (s), 1362 (s), 1313 (m), 1257 (m), 1183 (m), 903 (m), 784 (m), 677 (w), and 629 (w) cm^{-1} .

Crystallographic Data Collection and Refinement

Crystallographic data were collected with a Bruker SMART CCD diffractometer operating at room temperature. Intensities were collected with graphite monochromatized Mo-K α radiation ($\lambda = 0.71073 \text{ \AA}$), using the *phi* and *omega* scan technique. Data reduction was made with the Bruker SAINT package. Absorption correction was performed using the SADABS program. The structure was solved by direct methods and refined on F^2 by full-matrix least-squares using SHELXL-2000 with anisotropic displacement parameters for all non-hydrogen atoms. Hydrogen atoms were introduced in calculations using the riding model. All computations were carried out using the SHELXTL-2000 program package.^[20] The crystallographic data for **1**: C₂₀H₂₈Mn₃N₄O₂₂, M_r = 841.28, triclinic, space group $P\bar{1}$, $a = 6.7694(13) \text{ \AA}$, $b = 10.426(2) \text{ \AA}$, $c = 11.446(2) \text{ \AA}$, $\alpha = 70.626(2)^\circ$, $\beta = 75.957(2)^\circ$, $\gamma = 78.696(2)^\circ$, $V = 733.4(2) \text{ \AA}^3$, $Z = 1$, $F(000) = 427$, $\mu = 1.377 \text{ mm}^{-1}$, $D_c = 1.905 \text{ g}\cdot\text{cm}^{-3}$, GOF = 1.067, $R_1 = 0.0412$, $wR_2 = 0.0905$ [$I > 2\sigma(I)$]. Selected bond lengths, angles, and hydrogen bonds are listed in Table 1 and Table 2.

Crystallographic data for the structure reported in the paper has been deposited as supplementary publication CCDC-780182 for **1**. These data can be obtained free of charge via www.ccdc.cam.ac.uk/data_request/cif or from the Cambridge Crystallographic Data Centre CCDC, 12 Union Road, Cambridge CB2 1EZ, UK (Fax: 44-1223-336-033; or E-Mail: deposit@ccdc.cam.ac.uk).

Supporting Information (see footnote on the first page of this article): IR spectrum (Figure S1) and thermogravimetric analysis of **1** (Figure S2).

Acknowledgement

This work was supported by the National Natural Science Foundation of China (No. 20901049 and 20871095), Excellent Youth Teachers Foundation of Shanghai Municipal Education Committee and the Innovation Foundation of Shanghai University.

References

- [1] Y. Wei, Y. Yu, K. Wu, *Cryst. Growth Des.* **2008**, *8*, 2087.
- [2] Y. Yao, Y. Che, J. Zheng, *Cryst. Growth Des.* **2008**, *8*, 2299.
- [3] Y. Wei, Y. Yu, R. Sa, Q. Li, K. Wu, *CrystEngComm* **2009**, *11*, 1054.
- [4] Y.-R. Liu, L. Li, T. Yang, X.-W. Yu, C.-Y. Su, *CrystEngComm* **2009**, *11*, 2712.

- [5] F.-P. Huang, J.-L. Tian, D.-D. Li, G.-J. Chen, W. Gu, S.-P. Yan, X. Liu, D.-Z. Liao, P. Cheng, *CrystEngComm* **2010**, *12*, 395.
- [6] Y. Xie, Y.-H. Xing, Z. Wang, H.-Y. Zhao, X.-Q. Zeng, M.-F. Ge, S.-Y. Niu, *Inorg. Chim. Acta* **2010**, *363*, 918.
- [7] Z.-Y. Li, J.-W. Dai, N. Wang, H.-H. Qiu, S.-T. Yue, Y.-L. Liu, *Cryst. Growth Des.* **2010**, *10*, 2746.
- [8] Z.-X. Wang, Q.-F. Wu, H.-J. Liu, M. Shao, H.-P. Xiao, M.-X. Li, *CrystEngComm* **2010**, *12*, 1139.
- [9] Y. L. Lo, W. C. Wang, G. A. Lee, Y. H. Liu, *Acta Crystallogr., Sect. E* **2007**, *63*, m2657.
- [10] Q. Gao, W.-H. Gao, C.-Y. Zhang, Y.-B. Xie, *Acta Crystallogr., Sect. E* **2008**, *64*, m928.
- [11] M.-S. Liu, Q.-Y. Yu, Y.-P. Cai, C.-Y. Su, X.-M. Lin, X.-X. Zhou, J.-W. Cai, *Cryst. Growth Des.* **2008**, *8*, 4083.
- [12] K. Nakamoto, *Infrared and Raman Spectra of Inorganic and Co-ordination Compounds*, John Wiley and Sons, New York, **1997**.
- [13] L. Cañillas-Delgado, O. Fabelo, J. Cano, J. Pasán, F.-S. Delgado, F. Lloret, M. Julve, C. Ruiz-Pérez, *CrystEngComm* **2009**, *11*, 2131.
- [14] Z.-X. Wang, X.-L. Li, T.-W. Wang, Y.-Z. Li, S. Ohkoshi, K. Hashimoto, Y. Song, X.-Z. You, *Inorg. Chem.* **2007**, *46*, 10990.
- [15] Y.-G. Sun, W. Yu, L. Wang, S.-T. Rong, Y.-L. Wu, F. Ding, W.-Z. Zhang, E.-J. Gao, *Inorg. Chem. Commun.* **2010**, *13*, 479.
- [16] X.-Y. Wang, S. C. Sevov, *Chem. Mater.* **2007**, *19*, 3763.
- [17] E. Coronado, J. R. Galán-Mascarós, C. Martí-Gastaldo, J. C. Waerenborgh, P. Gaczyński, *Inorg. Chem.* **2008**, *47*, 6829.
- [18] K. Kambe, *J. Phys. Soc. Jpn.* **1950**, *5*, 48.
- [19] W.-Y. Wu, Y. Song, Y.-Z. Li, X.-Z. You, *Inorg. Chem. Commun.* **2005**, *8*, 732.
- [20] Bruker, *SMART, SAINT, SADABS, SHELLXTL*, Bruker AXS Inc., Madison, WI, USA, **2000**.

Received: July 27, 2010

Published Online: November 19, 2010